

Angular and range interferometry to refine weather radar resolution

Guifu Zhang

School of Meteorology, University of Oklahoma, Norman, Oklahoma, USA

Research Applications Laboratory, National Center for Atmospheric Research, Boulder, Colorado, USA

Tian-You Yu

School of Electrical and Computer Engineering, University of Oklahoma, Norman, Oklahoma, USA

Richard J. Doviak

National Severe Storms Laboratory, Norman, Oklahoma, USA

Received 20 July 2004; revised 24 November 2004; accepted 17 February 2005; published 22 June 2005.

[1] A weather radar's resolution volume is generally determined by beam and pulse widths. Recently, a single-antenna interferometric technique was developed to measure cross-beam and radial wind using angular and range interferometry. Here it is shown that the interferometry technique can refine radar resolution. The technique for resolution refinement is based on the fact that the cross-correlation function of signals from two resolution volumes is contributed only by scatterers in the shared volume. Therefore all the radar measureables derived from cross-correlation estimates have a resolution of the shared volume size rather than a radar-resolution volume size. The performance of the technique depends on the shape of beam/range-weighting functions and relative sample error. A sharp change at the edges of the weighting function and low sidelobes are important for resolution refinement using weather radar interferometry.

Citation: Zhang, G., T.-Y. Yu, and R. J. Doviak (2005), Angular and range interferometry to refine weather radar resolution, *Radio Sci.*, 40, RS3013, doi:10.1029/2004RS003125.

1. Introduction

[2] Weather radar's cross- and along-range resolutions are determined by antenna size and transmitted pulse width/receiver bandwidth respectively [Doviak and Zrnic, 1993, section 4.4.4]. Improving angular resolution by increasing antenna size is limited by cost constraints, whereas improving range resolution by increasing bandwidth and decreasing pulse width is often limited by Federal Communications Commission (FCC) regulations.

[3] Existing angular resolution refinement techniques include coherent processing methods such as the monopulse radar, Doppler Beam Sharpening (DBS), developed by Wiley in the early 1950s [Ulaby *et al.*, 1982, section 9–2], and an incoherent deconvolution method [Andrews and Hunt, 1977; Magain *et al.*, 1998]. The monopulse radar improves the resolution of a discrete

(point) scatterer's location within the radar's resolution volume V_6 [Doviak and Zrnic, 1993, section 4.4.4]. DBS, a Synthetic Aperture Radar (SAR) method, applies to a distribution of scatters fixed on a surface, but obliquely observed with an elevated moving antenna. The deconvolution method applies to a volumetric distribution of scatterers and improves resolution by separating the effects of a known antenna pattern on measured gradients of the reflectivity field. However, deconvolution is an ill-posed problem, and has no unique solution, especially in the presence of noise [Magain *et al.*, 1998]. Furthermore, sampled data can be perfectly deconvolved only if the sampling theorem, applied to the true reflectivity field, is not violated. Therefore various optimization techniques, such as a compensating filter [Andrews and Hunt, 1977; Palmer *et al.*, 1998; Yu and Palmer, 2001], are used to improve the result. However, the various optimization techniques do not work well for radar observations of weather in the presence of noise [Sadjadi, 2000].

[4] Weather Radar Interferometry (WRI) is a method whereby the cross correlation of two or more time series

of weather signals from a pair or more of overlapping V_6 s is used to extract meteorological information. For example, WRI is used to cross-correlate signals from overlapped bistatic V_6 s [Doviak and Zrnic, 1993, section 11.3] to measure cross-beam wind [Briggs *et al.*, 1950; Doviak *et al.*, 1996]. Zhang *et al.* [2003b] have extended the WRI technique to measure the cross-beam and radial wind components using overlapped resolution volumes of a monostatic radar. Herein WRI is applied to signals from overlapped V_6 s to refine weather radar resolution without increasing bandwidth or antenna diameter. WRI requires relatively high correlation and many samples of signals from overlapped V_6 s; this in turn requires radar with beam agility. The rapid and flexible scan capability of phased array antennas, such as that used by the National Weather Radar Testbed (NWRT) being developed at National Severe Storms Laboratory (NSSL), could provide this required capability, and opens opportunities to verify the theories for refinements in resolution and measurements of cross-beam winds using WRI.

[5] A conceptual description of the WRI technique for resolution refinement is presented in section 2. Beam splitting to further sharpen the beam is described in section 3. Numerical simulations are presented in section 4 to demonstrate how Angular Interferometry (AI) increases angular resolution and Range Interferometry (RI) improves range resolution. Finally, the feasibility for practical application is discussed in the summary.

2. Conceptual Description and Formulation

[6] Weather radars often measure hydrometeor characteristics, such as reflectivity factor, Z , and Doppler velocity v , through estimation of the temporal autocorrelation function obtained from a time series of weather signal samples spaced a Pulse Repetition Time (PRT) apart [Doviak and Zrnic, 1993, chapter 6]. Strictly speaking, measurements of hydrometeor characteristics are obtained from estimates of the *angular* autocorrelation function with sample spacing determined by the antenna's speed of rotation and the PRT. If the density of scatterers is homogeneous over the angular displacement of the beam, the angular autocorrelation can be treated as a temporal autocorrelation from a volume having an angular width larger than the beam width [Doviak and Zrnic, 1993, section 7.8].

[7] WRI for resolution refinement is based on the fact that the cross-correlation function of signals from two distinctly spaced but overlapping resolution volumes has, on average, contributions principally from those scatterers in the shared or overlapped volume. Consider two radar resolution volumes, $V_6(1)$ and $V_6(2)$, that are partially overlapped as shown in Figure 1, and N scatterers spread uniformly over the entire domain, but K of those are within the shared region. The weather

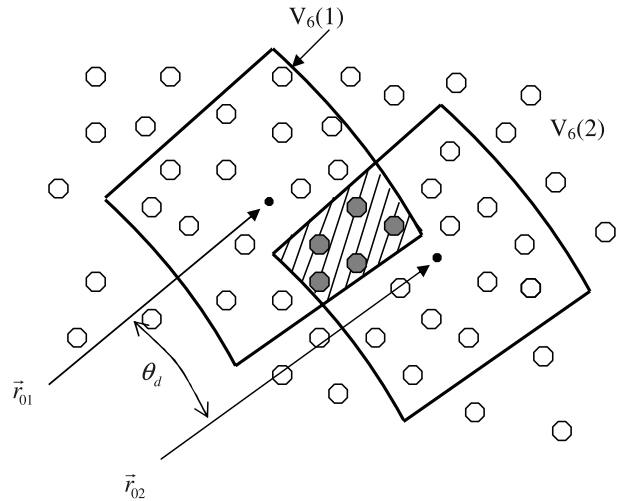


Figure 1. Configuration sketch of an interferometry technique for resolution refinement. See color version of this figure in the HTML.

signal is the sum of signals returned from each scatterer. Thus the weather signal voltage $V(\vec{r}_{01}, t_1)$ for $V_6(1)$ is proportional to [Doviak and Zrnic, 1993, section 4.2],

$$V(\vec{r}_{01}, t_1) \propto \sum_n^N A_{1n} W_{1n} e^{-j2kr_n(t_1)}, \quad (1)$$

and for $V_6(2)$ it is

$$V(\vec{r}_{02}, t_2) \propto \sum_n^N A_{2n} W_{2n} e^{-j2kr_n(t_2)}, \quad (2)$$

where A_{1n} is the prefilter, echo amplitude of the n th scatterer located at $\vec{r}_n(t_1)$ at time t_1 , \vec{r}_{01} is the location of the center of $V_6(1)$, and W_{1n} is a range-dependent weight, a function of the transmitted pulse width and the receiver filter's bandwidth. Similar definitions apply to (2). A_{1n} is proportional to the normalized radiated power density pattern $f^2(\theta - \theta_{01}, \phi - \phi_{01})$ of the antenna ($f^2(\theta, \phi)$ is also the two-way pattern gain function of the electric field) as well as the backscattering cross section of the scatterer. Because the range extent of V_6 is usually small compared to r_0 the small changes in the weighting function $W(r)$ due to the $1/r^2$ factor can be ignored.

[8] To apply WRI to refine angular resolution it is assumed that the location of V_6 is alternately switched between $V_6(1)$ and $V_6(2)$ in a Pulse Repetition Time (PRT $\equiv T_s$). There is no need to account for changes in A_{1n} due to changes in scatterer location because hydrometeors move, during a PRT, a short distance compared to the typical size of V_6 . However, the phase term can have considerable change because scatterers can move an

appreciable fraction of the wavelength during a PRT. Nevertheless, to illustrate the technique and to keep the development simple, differential phase shifts during the PRT are assumed to be negligible (i.e., it is assumed that $|r_n(t_1 + \text{PRT}) - r_n(t_1)| \ll \lambda/4\pi$ for all n). In other words, it is assumed that the PRT $\ll \tau_c$, the correlation time.

[9] Typically, weather signals can be considered to be statistically stationary during the data acquisition or dwell time T_d . Thus the cross-correlation function associated with signals from the two spaced resolution volumes can be written as

$$C_{12}(t_2 - t_1) = \langle V(\vec{r}_{01}, t_1) V^*(\vec{r}_{02}, t_2) \rangle = C_{12}(\tau), \quad (3a)$$

where brackets indicate time or ensemble averaging, and τ is sample lag spacing $\tau \equiv m\text{PRT} \equiv mT_s$. Therefore substituting from (1) and (2),

$$C_{12}(\tau) \propto \sum_n^N \sum_n^N \langle f^2(\vec{s}_{1n}) f^2(\vec{s}_{2n}) W(r_n, r_{01}) \cdot W^*(r_n, r_{02}) e^{-j2k[r_n(t) - r_n(t+\tau)]} \rangle, \quad (3b)$$

where $\vec{s}_{1n} \equiv (\theta_n - \theta_{01}, \phi_n - \phi_{01})$ is the angular position of the n th scatterer from the center of $V_6(1)$. Without losing the essence in explaining the WRI method, assume that the scatterers' cross sections are given unit weight if inside V_6 , but zero weight if outside. Thus the double sum in (3b) reduces to a single sum over the K scatterers within the shared volume, and (3b) reduces to

$$C_{12}(\tau) \propto \sum_n^K \langle e^{-j2k[r_n(t) - r_n(t+\tau)]} \rangle. \quad (3c)$$

There is no contribution to $C_{12}(\tau)$ from scatterers in the unshared region because, in this simplified example, either $f^2(\vec{s}_{1n})W(r_n, r_{01})$ or $f^2(\vec{s}_{2n})W(r_n, r_{02})$ is zero there. If two resolution volumes are displaced in angle (i.e., to refine angular resolution), the smallest τ could be is the PRT, and the beam would alternate between two closely spaced directions θ_d (Figure 1) every PRT. If the PRT is short (i.e., $T_s \ll \tau_c$) so that echoes from the two V_6 s are highly correlated, $|C_{12}(T_s)| \approx |C_{12}(0)|$ is proportional to the reflectivity within the shared volume. If the PRT is not short compared to τ_c , then the reflectivity would be obtained by interpolation to $|C_{12}(0)|$.

[10] Henceforth, to simplify our numerical simulations, it is assumed as stated earlier that $T_s \ll \tau_c$.

[11] Therefore measurements Z , v , etc. can be derived from $|C_{12}(T_s)|$ and are expressed as

$$Z \propto |C_{12}(T_s)| / \Delta V \quad (4)$$

$$v = \frac{\lambda}{4\pi T_s} \arg[C_{12}(T_s)] \quad (5)$$

with a resolution of the shared volume ΔV . Conventionally, Z , v , etc. are estimated from the autocorrelation function [Doviak and Zrnic, 1993], and the resolution is given by the size of V_6 .

[12] To refine range resolution, assume two resolution volumes displaced radially r_d (determined by range gate spacing), and assume r_d is less than the range resolution r_6 determined by the transmitted pulse width, τ_p , and the 6 dB bandwidth (B_6) of the receiver [Doviak and Zrnic, 1993, section 4.4.3]. If $B_6 \geq \tau_p^{-1}$, only scatterers inside the shared volume contribute significantly to $|C_{12}(r_d)|$.

[13] Using the above simplified example, it is seen how WRI can be used to refine resolution. In practice, however, the implementation is not as simple. Three main difficulties that limit the application of WRI for resolution improvement are as follows.

2.1. Limited Spatial and Temporal Bandwidths

[14] The weighting function, proportional to $f^2(\vec{s})W(r)$, does not have a rectangular form with zero weighting outside V_6 . A sharp change at the edges of the weighting function and low sidelobes are important for resolution refinement using WRI. For a simple illustration, consider two one-dimensional weighting functions (e.g., the one-way antenna power gain function proportional to $g(X - X_0)$) having a rectangular shape with centers separated by 1.0, and the product of these weighting functions (i.e., $g(X + 0.5)g(X - 0.5)$) as shown in Figure 2a. The product of the two weighting functions gives the shared region having half the width of the individual weighting functions.

[15] The rectangular function can be a good approximation for the range-weighting function if the transmitted pulse of width τ_p is rectangular, and $B_6 \gg \tau_p^{-1}$. However, a rectangular function is not a good representation of the antenna gain function. Therefore consider the usually assumed Gaussian shaped antenna patterns as shown in Figure 2b. It can be shown that the product of the two displaced gain patterns has the same width as each of the two individual gain functions squared! In the other words, cross-correlation estimates do not improve the resolution if the weighting function has a Gaussian form. The shape of the gain function and sidelobe levels, however, can be controlled by appropriate excitation of the array elements as shown in the next section. On the other hand, there is an inverse relation between low sidelobe levels and sharp edges of the antenna gain function; that is, narrow beams having sharper edges are usually obtained with uniformly excited elements, but at the cost of higher sidelobe levels.

2.2. Finite Sample Error

[16] Because perfect estimates of the correlation functions can only be obtained with an infinite number of

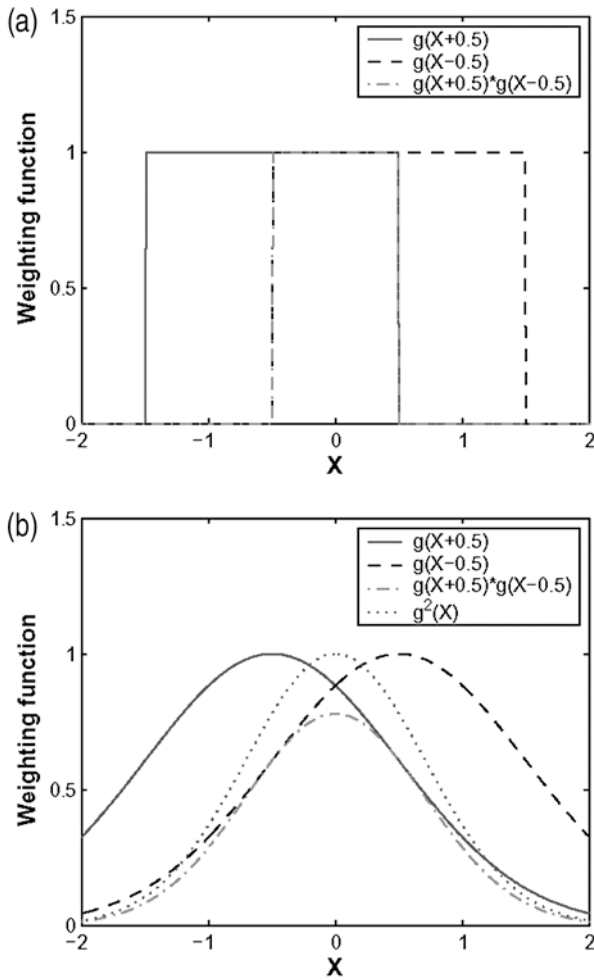


Figure 2. Effect of the gain function on resolution refinement: (a) rectangular weighting functions and (b) Gaussian weighting functions. See color version of this figure in the HTML.

samples (assuming the weather is statistically stationary), errors are incurred when a finite number of samples are processed. However, these relative errors (actually variance of the estimates) are larger for cross-correlation estimates than for autocorrelation estimates as is now shown. It is known that signal power estimates, \hat{S} (i.e., the autocorrelation function estimate at zero lag) have a relative Standard Deviation SD given by [Doviak and Zrnic, 1993]

$$\frac{SD(\hat{S})}{S} = \frac{1}{\sqrt{M_I}}, \quad (6)$$

whereas the relative SD for estimates of the cross-correlation function magnitude is [Zhang *et al.*, 2003a]

$$\frac{SD[|\hat{C}_{12}|]}{|C_{12}|} = \frac{1}{\sqrt{2M_I}} \left(1 + \frac{S^2}{|C_{12}|^2} \right)^{1/2}, \quad (7)$$

where M_I is the number of independent samples. Obviously, (7) is larger than (6) because $S/|C_{12}| > 1$ where S is the signal power from scatterers including those outside the shared volume. Scatterers outside the shared volume do not contribute the expected cross-correlation magnitude, but do contribute to S and thus to the SD of the cross-correlation estimates. In other words, signals from scatterers outside the shared volume are unwanted causing a larger relative standard deviation. Echoes from scatterers outside the shared resolution volume form two relatively independent streams of weather signals. One stream is associated with the scatterers weighted with $f^2(\vec{s}_{1n})W(r_n, r_{01}) \equiv W_1$, and a second stream is associated with echoes from the same scatterers but weighted with the function $f^2(\vec{s}_{2n})W(r_n, r_{02}) \equiv W_2$. Because W_1 and W_2 significantly weight different regions of scatterers, and because the scatterers' locations are independent of one another, the two echo streams will be relatively independent. The signal level associated with these two streams, however, is of comparable level to the signal coming from the shared volume. For example, if the weighting function is rectangular and half of the function is overlapped and the scatterers are uniformly distributed, the RMS level of the signal associated with scatterers outside the shared volume would be equivalent to the RMS level of signals coming from the shared volume. Nevertheless, the increased SD of the cross-correlation estimates can be diminished by increasing the dwell time, or equivalently M_I .

2.3. Relative Noise Power

[17] WRI can have a lower effective signal-to-noise ratio (SNR) because $|C_{12}| < S$. It is true that the noise contribution to the variance of the cross-correlation estimates is smaller than that to autocorrelation estimates as shown by (12) and (13) of Zhang *et al.* [2004]. However, the first-order noise term decreases from $\frac{N}{M}(S + |C_{11}(2\tau)|)$ to $\frac{NS}{M}$, and the second-order term decreases from $\frac{N^2}{2M}(1 + \delta(\tau))$ to $\frac{N^2}{2M}$. However, such decreases in the noise terms are limited by the reduced cross-correlation magnitude. For example, if $S/|C_{12}| > 2$ (i.e., less than one half the resolution

volume shared), the WRI has a lower SNR compared to the SNR associated with auto-correlation processing.

3. Beam Splitting

[18] As shown in the previous section, sharp edges of the antenna gain function are desirable in using WRI to refine angular resolution. However, a rectangular pattern cannot be obtained with an antenna of finite size; that requires a current distribution having the form $\sin(x)/x$ vs $x: [-\infty, +\infty]$. The narrowest beam and sharpest edges are obtained if the current distribution is uniform across a finite array. Nevertheless a pair of sharper beams, each with higher resolution than a uniformly illuminated aperture, can be obtained by splitting the main lobe, a technique similar to that used in the formation of the receiving beam of monopulse radar like the AN/SPY-1. The NWRT being developed at NSSL uses an AN/SPY-1 phased array antenna (Figure 3a). Figure 3b shows the antenna pattern for the monopulse sum (i.e., the transmitted radiation pattern), and Figure 3c shows the monopulse elevation difference pattern used for reception. As can be seen, the individual beams of the difference pattern (i.e., split beams) are about 25% narrower than that of a sum pattern. Considering the cost of an antenna is at least proportional to the square of its diameter, a 25% improvement in the angular resolution could produce a cost savings of nearly 50% or more.

[19] The gain pattern is determined by antenna size and distribution of the current's magnitude and phase across the aperture. To illustrate the improvement of angular resolution provided by beam splitting we consider, for sake of simplicity, one-dimensional arrays and the following three current distributions:

(1) uniform magnitude and phase

$$I_1(x) = I_0 \quad (-D/2 < x < D/2), \quad (8)$$

(2) uniform magnitude but antisymmetric phase distribution

$$I_2(x) = \begin{cases} I_0 & (0 < x < D/2) \\ -I_0 & (-D/2 < x < 0), \end{cases} \quad (9)$$

and (3) a linear distribution of current

$$I_3(x) = 4I_0x/D \quad (-D/2 < x < D/2). \quad (10)$$

The electric field-weighting function $f(\theta)$ is the Fourier transform of the current distribution [Ishimaru, 1991, section 9-4], that is,

$$f(\theta) = \int_{-D/2}^{D/2} I(x)e^{jkx \sin \theta} dx, \quad (11)$$

where θ is the elevation angle, and the beam axis is assumed to be at $\theta_{01} = 0^\circ$. Substitution of (8)–(10) into (11) yields the three corresponding field patterns:

$$f_1(\theta) = I_0D \frac{\sin(kD \sin \theta/2)}{kD \sin \theta/2} \quad (12)$$

$$f_2(\theta) = I_0D \frac{i}{kD \sin \theta/2} [1 - \cos(kD \sin \theta/2)] \quad (13)$$

$$f_3(\theta) = I_0D \frac{-2i}{kD \sin \theta/2} \cdot \left[\cos(kD \sin \theta/2) - \frac{\sin(kD \sin \theta/2)}{kD \sin \theta/2} \right]. \quad (14)$$

Figure 4a shows the current distributions, and Figure 4b shows the corresponding antenna power patterns normalized by $(I_0D)^2$ (i.e., $|f_1^{(n)}(\theta)|^2 = |f_1(\theta)|^2/(I_0D)^2$) for an antenna size of 3.66 m at a frequency of 3.2 GHz (i.e., the NWRT parameters). With opposite phase of the excitation current on each half of the antenna, the one-way power density pattern is split into two beams as shown by $|f_2^{(n)}(\theta)|^2$ and $|f_3^{(n)}(\theta)|^2$. The one-way half-power beam widths are 1.30° , 1.18° , and 1.01° , respectively. To achieve a 1° beamwidth with uniform illumination, the antenna diameter would have to be increased by about 30%, a costly solution. However, the sidelobe levels for $|f_3^2(\theta)|$ are significantly higher. For example, the normalized first sidelobe levels are: -13.3 , -10.6 , and -8.3 dB, respectively.

4. Numerical Simulations

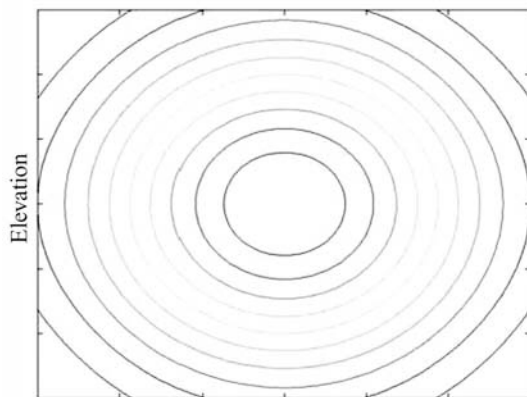
[20] In this section, we describe numerical simulations of wave scattering that are used to verify WRI for resolution refinement. In these simulations, the medium is modeled by a collection of randomly distributed scatterers. Again, for the sake of illustration, we consider a 1-D power density pattern.

4.1. Interferometry to Refine Angular Resolution

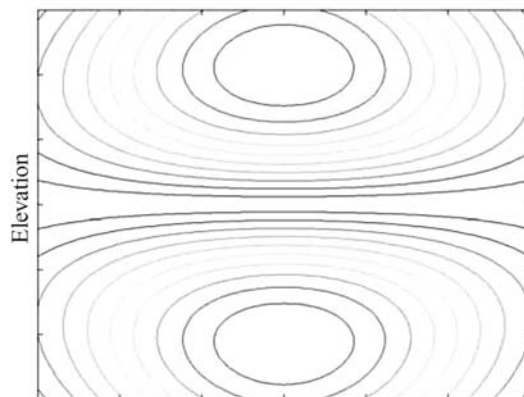
[21] Consider two layers of randomly distributed scatterers at a range of 50 km and separated by 800 m. The WRI technique is applied to a pair of overlapped antenna patterns, one pair for $f_1^2(\theta)$, and the other pair for the split beam pattern $f_3^2(\theta)$. WRI to refine angular resolution with split beams is achieved by alternately shifting beam directions such that only one of the split beams is overlapped with the other,



(a)



(b)



(c)

Figure 3. (a) NWRT's phased array antenna (i.e., the AN/SPY-1A) being covered with a radome (courtesy of Allen Zahrai, National Severe Storms Laboratory) and (b) transmit sum and (c) receive elevation difference voltage patterns of the AN/SPY-1A antenna (courtesy of Lockheed Martin Corp.). See color version of this figure in the HTML.

whereas angular refinement with $f_1^2(\theta)$ is obtained by over lapping the pair of main lobes. Range weighting is uniform over a 100 m interval, and within this range interval there are $N = 50$ scatterers in each layer

having a thickness of 10 m. The aim of refining the angular resolution using WRI is to resolve the two layers. At the 50 km range, the angular separation θ_{sc} of the two scattering layers is 0.92° . The weather

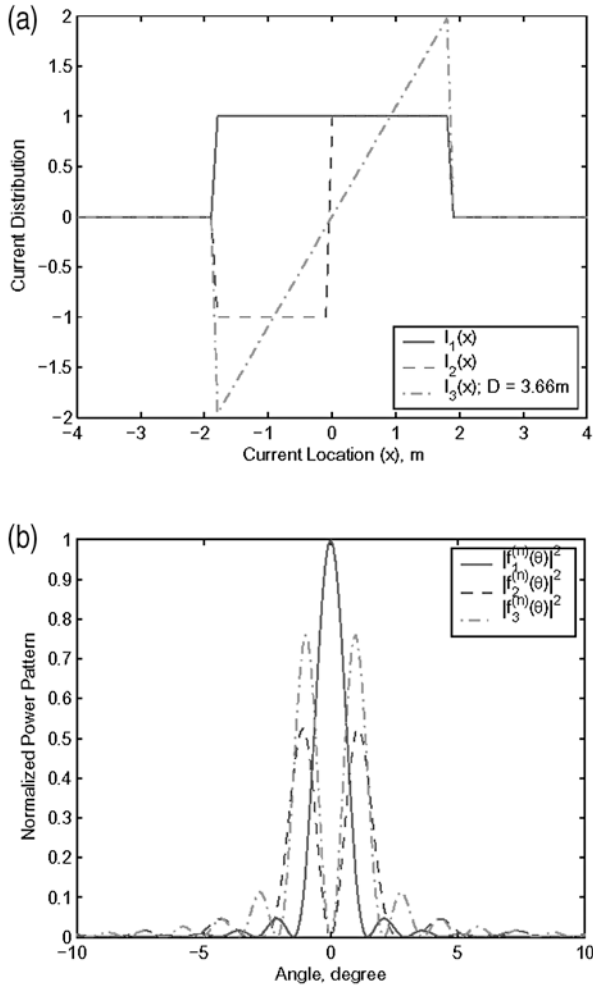


Figure 4. (a) Three examples of current distributions on linear antennas and (b) the corresponding radiation patterns. See color version of this figure in the HTML.

signal for each beam position of the pair can be expressed as

$$V(\theta, t) = \sum_{n=1}^N f^2(\theta_n - \theta) e^{2jkr_n(t)}, \quad (15)$$

where the center of V_6 is at $\theta = \theta_{01}$ for the first beam position (Figure 5), and $\theta = \theta_{02}$ for the second beam position (Figure 5), and θ_n is the angular location of the n th scatterer. Time series data pairs are obtained by randomly changing the scatterers' positions after alternately sampling the media with the two different beam directions; a total of two hundred pairs are realized to obtain $M = 200 = M_I$ independent estimates of $C_{12}(0)$; in real radar applications, the zero-lag cross-correlation function $C_{12}(0)$ can be approximated by the first-lag

cross-correlation function, that is, $C_{12}(0) \approx C_{12}(T_s)$, if $T_s \ll \tau_c$, or through interpolation. Both the single-beam pattern $f_1^2(\theta)$ and the split beam pattern $f_3^2(\theta)$ are used in the simulations. The cross-correlation function is then estimated from the time series data by averaging over M realizations to obtain

$$\begin{aligned} \hat{C}_{12}(\theta_{01}, \theta_{02}) &= \frac{1}{M} \sum_{m=1}^M V(\theta_{01}, t_m) V^*(\theta_{02}, t_m) \\ &\equiv \hat{C}_{12}(\theta_c, \theta_d), \end{aligned} \quad (16)$$

where $\theta_c = (\theta_{01} + \theta_{02})/2$ is the mean angular location, and $\theta_d = \theta_{02} - \theta_{01}$ is the angular separation of the two beam directions. When $\theta_d = 0$, $\hat{C}_{12} = \hat{C}_{11}$.

[22] The simulation results for the correlation coefficient estimates plotted as a function of θ_c are shown in Figure 6. Figure 6a shows the results for a single-beam pattern $f_1^2(\theta)$ with beam displacement θ_d as a parameter. Using autocorrelation estimates (i.e., $\theta_d = 0$; WRI is not used), the two layers of the scatterers can hardly be distinguished. However, using WRI and the cross-correlation estimates with $\theta_d \neq 0$ the two scattering groups are better resolved. However, the cross correlation is lower for larger separation, which means a lower SNR, a larger relative sampling error, and a higher sidelobe level.

[23] Figure 6b gives a similar presentation for the split beam pattern $f_3^2(\theta)$. The autocorrelation estimates give

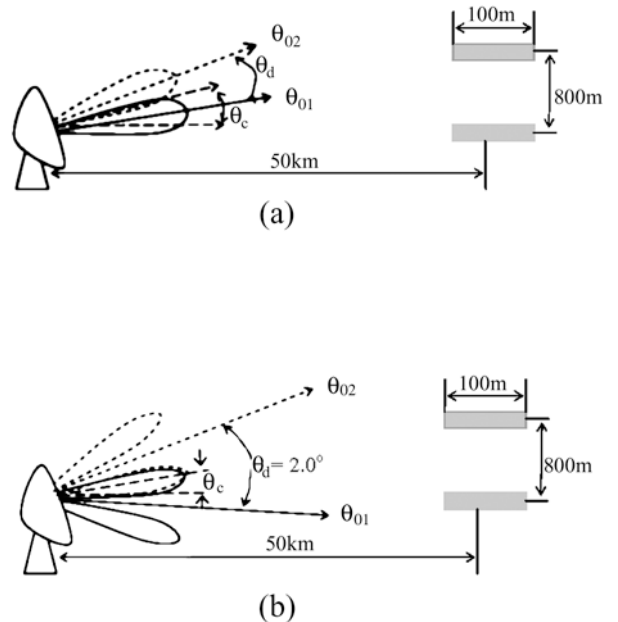


Figure 5. Configuration of antenna patterns to implement WRI to refine angular resolution: (a) single beam and (b) split beams.

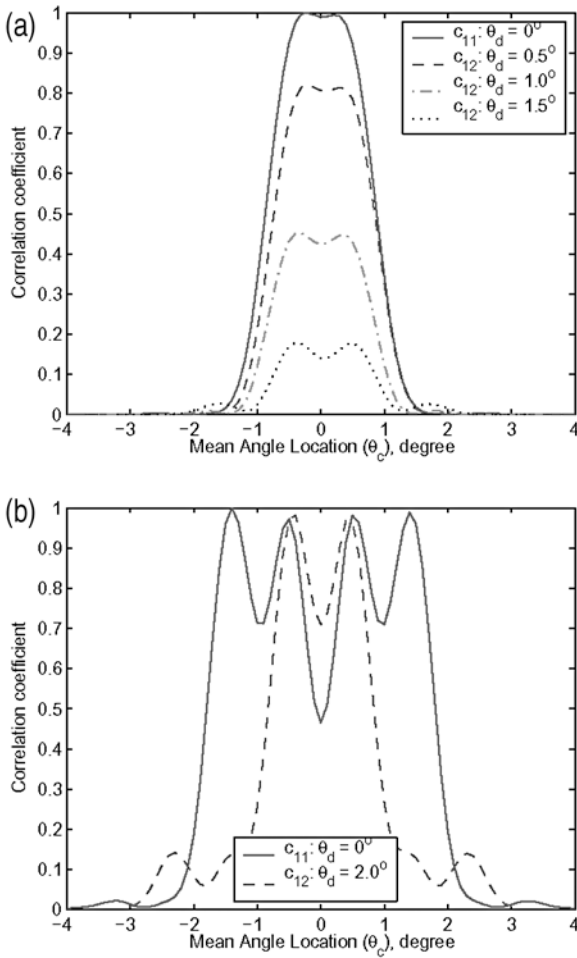


Figure 6. Monte Carlo simulations for interferometry to refine angular resolution: (a) uniform excitation/single beam and (b) linear distribution of excitation distribution/split beam. See color version of this figure in the HTML.

ghost images as each layer of scatterers are seen by the two main lobes of the split beam. On the other hand, the cross-correlation estimator with beam displacement $\theta_d = 2^\circ$ clearly distinguishes the two layers of scatterers while maintaining the same level of correlation magnitude.

4.2. Interferometry to Refine Range Resolution

[24] To demonstrate refinement of range resolution using WRI, consider two slabs, each with a thickness of 10 m, and placed at different ranges separated by 60 m as shown in Figure 7a. Each slab contains randomly distributed scatterers. The weather signal is calculated from

$$V(r, t) = \sum_{n=1}^N W(r_n - r) e^{2jkr_n(t)}, \quad (17)$$

where the resolution volume center is r , r_n is the range to the n th scatterer, $W(r)$ is the range-weighting function assumed to have a rectangular form with a resolution of 100 m. Then, the range cross-correlation function is estimated from the time series data $V(r_{01}, t)$, $V(r_{02}, t)$ by averaging over M realizations as

$$\begin{aligned} \hat{C}_{12}(r_{01}, r_{02}) &= \frac{1}{M} \sum_{m=1}^M V(r_{01}, t_m) V^*(r_{02}, t_m) \\ &\equiv \hat{C}_{12}(r_c, r_d), \end{aligned} \quad (18)$$

where $r_c = (r_{01} + r_{02})/2$ is the range to the center of the shared volume, and $r_d = r_{02} - r_{01}$ is the range separation of the two resolution volumes. When $r_d = 0$, \hat{C}_{12} becomes autocorrelation function estimate \hat{C}_{11} .

[25] The simulation results of correlation coefficient estimates are plotted in Figure 7b as a function of r_c . Autocorrelation estimation cannot separate the two

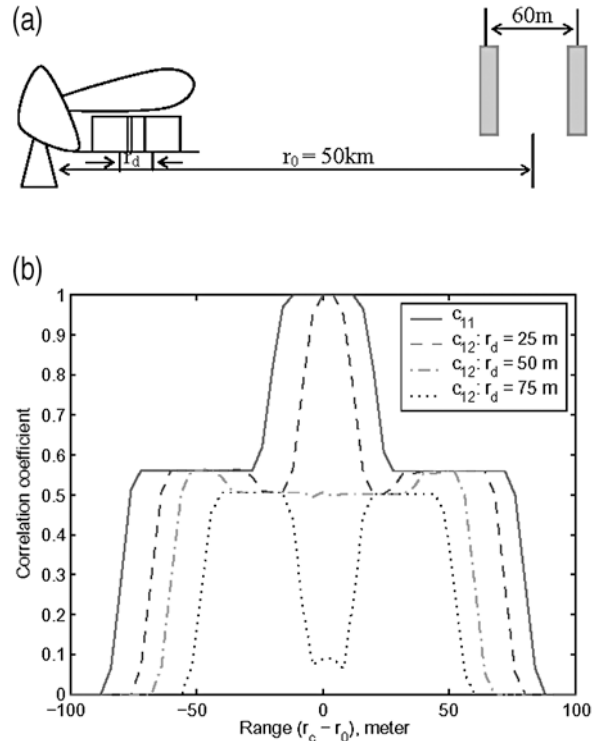


Figure 7. Monte Carlo simulations to demonstrate WRI to refine range resolution. Parameters used for simulations are a rectangular range-weighting function with a resolution of 100 m and a 60 m range separation for the two groups of scatterers. See color version of this figure in the HTML.

groups of scatterers, but WRI using the cross correlation estimated with a range separation of 75 m clearly distinguishes the two slabs of scatterers while it maintains a substantial level of correlation magnitude.

5. Summary and Discussions

[26] In this paper, we apply Weather Radar Interferometry (WRI) to refine weather radar resolution. The resolution refinement technique is described using the theory of wave scattering from a random medium. The WRI technique for resolution refinement is based on the fact that the most significant contribution to the cross-correlation function, of signals from two overlapping resolution volumes $V_6(1)$ and $V_6(2)$, is from scatterers in the shared volume. The shared volume for beam width refinement must be obtained by rapidly alternating, from transmitted pulse to transmitted pulse, the direction of the beam, and cross correlating the signals from the two overlapped beam directions.

[27] The difficulties for the practical application of WRI to refine resolution are: (1) a larger relative sampling error, (2) the requirement of a sharp change at the edges of the angular/range-weighting functions, (3) lower signal-to-noise ratio (SNR) than that associated with the commonly used autocorrelation techniques, and (4) higher sidelobe levels, especially for angular resolution refinement. The sampling error may be reduced using a larger number of independent samples. A sharp edge of the principal lobe of the antenna's radiation pattern can be achieved by splitting the beam as discussed in section 3. The lower SNR is difficult to overcome because the added noise originates from the scatterers outside the shared volume and thus the added noise increases in proportion to the level of signal from the shared volume. Worse yet, if the shared volume is made smaller to increase the resolution, the added noise increases which further increases the variance of the estimates of the cross-correlation function and, in turn, the estimates of reflectivity and Doppler velocity in the shared volume. Furthermore, the number of independent samples that can be used to reduce the added noise is typically much less than that number for receiver noise. The deleterious effects due to increased side lobe levels might be suppressed by using the switched antenna pattern technique described by Sachidananda et al. [1985].

[28] Numerical simulations were used to verify that range and angular resolutions of weather radars can be improved by cross-correlating signals from resolution volumes displaced in range and angle. The numerical results were based on single-lag estimates. They can be further improved by optimally combining multilag cross-correlation function estimates as shown by Backus and Gilbert [1970] and T. Yu et al. (Resolution enhancement

using range oversampling, submitted to *Journal of Atmospheric and Oceanic Technology*, 2004). By shifting the shared resolution volume, WRI can also be used to increase the number of independent samples. This latter application should be compared to the whitening transformation described by Torres and Zrníc [2003]. Although these preliminary results demonstrate resolution refinement for weather radar, further detailed studies (e.g., optimal inversion) are required to better define the limitations of the technique.

[29] **Acknowledgment.** The authors greatly appreciate helpful discussions with Dusan S. Zrníc, J. Vivekanandan, Jeff Keeler, Edward A. Brandes, Robert J. Serafin, and Akira Ishimaru and the support provided by NCAR, NOAA, and the University of Oklahoma.

References

- Andrews, H. C., and B. R. Hunt (1977), *Digital Image Restoration*, Prentice-Hall, Upper Saddle River, N. J.
- Backus, G. E., and J. F. Gilbert (1970), Uniqueness in the inversion of inaccurate gross Earth data, *Philos. Trans. R. Soc. London*, 266, 123–192.
- Briggs, B. H., G. J. Phillips, and D. H. Shinn (1950), The analysis of observation on spaced receiver of the fading radio signals, *Proc. Phys. Soc. London, Sect. B*, 63, 106–121.
- Doviak, R. J., and D. S. Zrníc (1993), *Doppler Radar and Weather Observations*, 2nd ed., 562 pp., Elsevier, New York.
- Doviak, R. J., R. J. Latatits, and C. L. Holloway (1996), Cross correlations and cross spectra in spaced antenna wind profilers: 1: Theoretical analysis, *Radio Sci.*, 31, 157–180.
- Ishimaru, A. (1991), *Electromagnetic Wave Propagation, Radiation and Scattering*, 637 pp., Prentice-Hall, Upper Saddle River, N. J.
- Magain, P., F. Courbin, and S. Sohy (1998), Deconvolution with correct sampling, *Astrophys. J.*, 494, 472–477.
- Palmer, R. D., S. Gopalam, T.-Y. Yu, and S. Fukao (1998), Coherent radar imaging using Capon's method, *Radio Sci.*, 33, 1185–1198.
- Sachidananda, M., R. J. Doviak, and D. S. Zrníc (1985), Whitening of sidelobe powers by pattern switching in radar array antenna, *IEEE Trans. Antennas Propag.*, 33(7), 727–735.
- Sadjadi, F. (2000), Radar beam sharpening using an optimum FIR filter, *Circuits Syst. Signal Process.*, 19(2), 121–129.
- Torres, S. M., and D. Zrníc (2003), Whitening of signals in range to improve estimates of polarimetric variables, *J. Atmos. Oceanic Technol.*, 20, 1776–1789.
- Ulaby, F. T., R. K. Moore, and A. K. Fung (1982), *Microwave Remote Sensing: Active and Passive*, vol. 2, *Radar Remote Sensing and Surface Scattering and Emission Theory*, Artech House, Norwood, Mass.

- Yu, T., and R. D. Palmer (2001), Atmospheric radar imaging using multi-receiver and multiple-frequency technique, *Radio Sci.*, 36, 1493–1503.
- Zhang, G., R. J. Doviak, J. Vivekanandan, W. O. J. Brown, and S. A. Cohn (2003a), Cross-correlation ratio method to estimate cross-beam wind and comparison with a full correlation analysis, *Radio Sci.*, 38(3), 8052, doi:10.1029/2002RS002682.
- Zhang, G., R. J. Doviak, J. Vivekanandan, and T. Yu (2003b), Angular and range interferometry to measure wind, *Radio Sci.*, 38(6), 1106, doi:10.1029/2003RS002927.
- Zhang, G., R. J. Doviak, J. Vivekanandan, W. O. J. Brown, and S. A. Cohn (2004), Performance of correlation estimators for spaced-antenna wind measurement in the presence of noise, *Radio Sci.*, 39, RS3017, doi:10.1029/2003RS003022.
-
- R. J. Doviak, National Severe Storms Laboratory, 1313 Halley Circle, Norman, OK 73069, USA.
- T.-Y. Yu, School of Electrical and Computer Engineering, University of Oklahoma, Norman, OK 73019, USA.
- G. Zhang, Research Applications Laboratory, National Center for Atmospheric Research, P.O. Box 3000, Boulder, CO 80307, USA. (guzhang@ucar.edu)